EUROPEAN FUSION DEVELOPMENT AGREEMENT

EFDA–JET–CP(01)02-85

D. Testa, F. Zonca, S. Briguglio, L. Chen, S. Dettrick,
A. Fasoli, A. Gondhalekar, G. Vlad
and JET EFDA Contributors

Energetic Particle Modes in JET Optimized Shear Experiments with non-Monotonic q-Profiles

Energetic Particle Modes in JET Optimized Shear Experiments with non-Monotonic q-Profiles

D. Testa[1], F. Zonca[2], S. Briguglio[2], L. Chen[3], S. Dettrick[3],
A. Fasoli[1], A. Gondhalekar[4], G. Vlad[2]
and JET EFDA Contributors*

[1]*Plasma Science and Fusion Center, Massachusetts Institute of Technology, Boston, USA.*
[2]*Associazione EURATOM-ENEA sulla Fusione, C.P.65, 00044-Frascati, Italy.*
[3]*Department of Physics, University of California at Irvine, USA.*
[4]*Euratom — UKAEA Fusion Association, Culham Science Center, Abingdon, UK.*
**See appendix of the paper by J.Pamela "Overview of recent JET results",*
Proceedings of the IAEA conference on Fusion Energy, Sorrento 2000

Preprint of Paper to be submitted for publication in Proceedings of the
EPS Conference,
(Madeira, Portugal 18-22 June 2001)

EXPERIMENTAL OBSERVATIONS

A new class of instabilities in the Alfvén frequency range, excited by ICRF-driven fast ions, is observed during the current ramp-up phase of JET Optimized Shear (OS) plasmas with a nonmonotonic q-profile. Fig. 1 shows a typical example of such measurements.

These n=1-7 Alfvénic modes observed in OS plasmas with non-monotonic q-profile do not follow the scaling $f(t) \propto B/q\sqrt{n_i}+nf_{\phi TOR}$ typical of the ICRF-driven TAEs which appear in JET plasmas with monotonic q-profile. The modes originate in the Alfvén continuum around r/a≈0.2 at f≈20÷50kHz, and saturate after ≈100÷400ms in the TAE gap at $f \approx f_{TAE}(q_{MIN})$ around $r/a=r/a(q_{MIN}) \approx 0.5$. The chirping rate is proportional to the toroidal mode number, $df/dt \propto n$, and is independent on m.

SIMULATIONS AND THEORETICAL ANALYSIS OF EPM EXCITATION AND DIFFUSIVE FAST ION TRANSPORT

We analyze JET Pulse No: 49382 in the time interval 3.5<t(s)<4 to discuss EPM excitation by ICRF driven fast ions [4-7] and the relation of the EPMs with other Alfvén modes [8]. The minority hydrogen fast ion population can be modeled [1,2] using a bi-Maxwellian distribution function, with $T_{\perp H}/T_{\parallel H} \approx 10$. The fast ions have potato orbits, $\omega_{orbit} << \omega_{precession}$ [3]. The plasma parameters are $R_0/a=3.13$, $B_0=2.6T$, $n_{e0}=1.6\times10^{19}m^{-3}$, $n_H/n_D=0.04$, $v_{H,max}/v_{A0}=0.45$, $\rho_{*H}=1.9\times10^{-2}$, $T_{\perp H}=210keV$, $\beta_{i0}=0.2\%$, $\beta_{e0}=0.43\%$, $\beta_{H0}=0.8\%$. Radial profiles for q and β are given in Fig.2; Fig.3 gives those for the magnetic shear s=rq'/q and $\alpha_H=-R_0q^2(d\beta_H/dr)$. This gives an indication of the strength of the fast ion drive on the EPMs, which is strongest at r/a≈0.2, as shown in Fig.2.

Numerical 1D-GK linear simulations confirm this expectation [7], as shown in Fig.4. The mode is identified as a resonantly excited EPM and not as a TAE due to the strength of the growth rate, which is comparable with the gap width [7]. Non-linear simulations, using a 3D hybrid MHD-GK code [9], demonstrate strong resonant excitations of an EPM around r/a=0.2, where the resonant drive is maximum. For the simulations, β_H has been rescaled such that α_H is constant, a/R=0.1, and the fast ion energy distribution function is taken as a Maxwellian.

Figure 5 shows that, after a transient phase, an unstable EPM appears at r/a≈0.3, causing rapid fast ion radial transport. The mode structure evolves as the fast ion source is radially displaced and weakened. The mode then merges into an Alfvén mode near the TAE gap at the position of the q-minimum surface at r/a≈0.49, as shown in Fig.6. This rapid nonlinear evolution takes place on a time scale of $\approx 100\tau_A$ and explain also why experimental observations of mode frequencies fit well with those of shear Alfvén waves localized near the q-minimum surface [8]. These modes have been recently interpreted as a variety of Global Alfvén Modes (GAE) [10] that exist near the local maximum of the Alfvén continuum at a q-minimum surface [8].

We consider now modes localized near r_0 (here $r_0/a=0.49$), where q has a minimum given by q_0. The toroidal and poloidal mode numbers (n,m) are such that the normalized parallel wave vector are $\Omega_{A,m}=nq_0-m<0$ and $\Omega_{A,m-1}=nq_0-m+1>0$. Continuum damping is minimized for $-1/2<\Omega_{A,m}<0$

and $1/2 < \Omega_{A,m} < 1$. This is the condition for a frequency gap in the continuum between the (m,n) mode, with a local maximum at r_0, and the (m−1,n) mode, with a local minimum at r_0.

For high-n's, no GAE [10] exist near an extremum of the Alfvén continuum, since the effect of the equilibrium current scales as'$1/n$. Fast ions may also provide this localization effect. To show this, we start from eq.(23) of [6] that, for the (m,n) mode reads

$$\left\{(e_\theta - e_r\xi) \bullet \left[\Omega^2 - \Omega^2_{A,m}\left(1+\frac{x^2}{\Omega_{A,m}}+\frac{x^4}{4\Omega^2_{A,m}}\right)\right] \bullet (e_\theta - e_r\xi) + \Lambda_m\right\}\delta\psi_m = 0, \tag{1}$$

Here $\Omega = \omega/\omega_A = qR_0\omega/\upsilon_A$, $x = [n(\partial^2 q/\partial r^2)_{r0}]^{1/2}(r-r_0)$, $\xi = (i\sqrt{n})S(\partial/\partial x)$, $S = (r_0/q_0)[(\partial^2 q/\partial r^2)_{r0}]^{1/2}$, and a similar equation can be written for the (m-1,n) mode. The term Λ_m in eq.(1) represents the fast ion contribution, whose non-resonant response can be approximated for $\omega_d >> \omega_b >> \omega$ as [6]

$$\Lambda_m = -\frac{q^2R_0^2}{m^2/r_0^2}\frac{4\pi w}{c}\frac{e^2}{m_H}\left\langle J_0^2(\lambda_H)QF_{0H}\right\rangle, \quad (2) \quad \lambda_H = k_\perp \nu_\perp/\omega_{cH},\ Q = (2\omega\partial/\partial\nu^2 + k\times b\bullet\nabla/\omega_{cH}).$$

Here F_{0H} is the fast hydrogen tail distribution function and we have assumed deeply trapped potato orbits [3], for which the mode drive is expected to be strongest. For $\Omega_{A,m} + \Omega_{A,m-1} >> r_0/R$, toroidal coupling between (m,n) and (m−1,n) modes can be neglected. The two modes, then, satisfy the following approximate dispersion relations, derived from a variational principle [6]:

$$\sqrt{\Omega_{A,m}+\Omega} - \frac{S\pi}{2^{5/2}n^{1/2}}\left(\frac{2n}{S^2}\frac{\Lambda_m}{\Omega_{A,m}} - 1\right) = 0, \qquad \sqrt{\Omega_{A,m-1}-\Omega} - \frac{S\pi}{2^{5/2}n^{1/2}}\left(\frac{2n}{S^2}\frac{\Lambda_{m-1}}{\Omega_{A,m-1}} - 1\right) = 0, \tag{3}$$

where $\Lambda_{m-1} \approx \Lambda_m < 0$. Furthermore, $\Lambda_{m-1} \approx \Lambda_m < 0$ since $\omega_d >> \omega_b >> \omega$: thus, the fast ions behave as nearly massless and are characterized by negative compressibility, which causes an upward shift in the mode frequency, contrary to the general case for which fast ion compression shifts the mode frequency downward [4,6,7]. For this reason, only the (m,n) mode can exist just above the local maximum of the Alfvén continuum at r_0, but not the (m−1,n) mode, just below the local minimum of the continuum. The condition for the existence of the (m,n) mode is $\Lambda_m/\Omega_{A,m} > S^2/2n$, which, as a consequence of Eq.(2) is independent on n and the mode frequency. This condition imposes a lower bound on the fast hydrogen tail density. For the present parameters, this gives $n_H/n_D > 3.1\%$, consistent with the experimental value $n_H/n_D \approx 4\%$. As $\Omega_{A,m} + \Omega_{A,m-1} \rightarrow 0^+$ (which may occur when, as in the experiment, q_0 drops), toroidal coupling effects become more important. Two branches are present as in Eq.(3), one of which strongly continuum damped (odd mode); the other (even mode) satisfies the modified dispersion relation [6]:

$$\left[\varepsilon_0^2\Omega^4 - (\Omega^2 - 1/4)\right]^{1/4} - \frac{S\pi}{2^{3/2}n^{1/2}}\left(\frac{2n}{S^2}\frac{\Lambda_m}{\Omega_{A,m}} - 1\right) = 0, \quad (4) \qquad \varepsilon_0 = 2(r_0/R+\Delta'),\ \Omega_{A,m} \approx -1/2$$

On the LHS of Eq.(4), the fourth root of the quantity in parentheses appears due to the local minimum in the q-profile, and not the square root as in the usual TAE case [6]. In both cases, the exponentially small continuum damping, due to the non-local interaction with the (m,n) mode continuum, and other kinetic damping mechanisms must be evaluated and compared with the resonant drive associated with fast ions before the existence of such modes is demonstrated on a rigorous basis. When $\Omega_{A, m} + \Omega_{A, m-1} << -r_0/R$, due to a further drop in q_0, the local interaction with the Alfvén continuum cannot be avoided for both (m,n) and (m−1,n) modes that are strongly damped. This explains why, after reaching the TAE frequency, the modes observed disappear.

ACKNOWLEDGEMENT
This work has been conducted under the European Fusion Development Agreement. D. Testa and A. Fasoli were partly supported by DoE contract No. DE-FG02-99ER54563.

REFERENCES
[1]. D.Testa et al., *Nucl. Fusion* 40, 975 (2000).
[2]. D.Testa et al., *Phys. Plasmas* 6, 3489 (1999); and *Phys. Plasmas* 6, 3498 (1999).
[3]. L.-G.Eriksson et al., *Plasma Phys Control. Fusion* 43, R145 (2001).
[4]. L.Chen, *Phys. Plasmas* 1, 1519 (1994).
[5]. F.Zonca et al., *Phys Fluids* B5, 3668 (1993).
[6]. F.Zonca et al., *Phys. Plasmas* 7, 4600 (2000).
[7]. L.-J. Zheng et al., *Phys. Plasmas* 7, 2469 (2000).
[8]. H.L.Berk et al., International Fusion Theory Conference, 2001, Santa Fe, USA, paper 1C54.
[9]. S.Briguglio et al., *Phys. Plasmas* 2, 3711 (1995); and *Phys. Plasmas* 5, 3287 (1998).
[10]. J.P.Goedbloed, Physica D 12, 107 (1984).

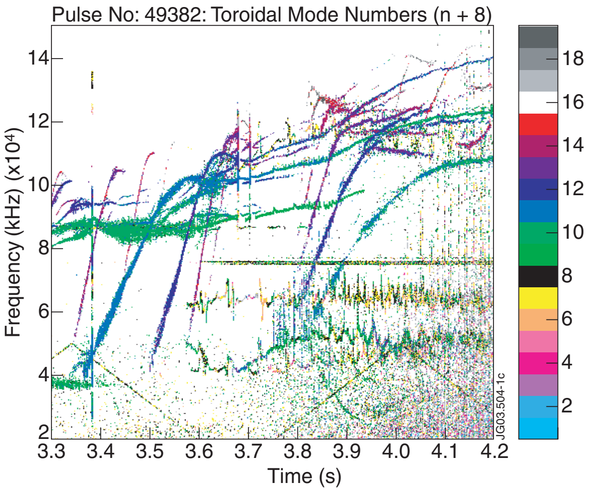

Figure 1: Magnetic spectrum in the preheating phase of an OS plasma with non monotonic q-profile.

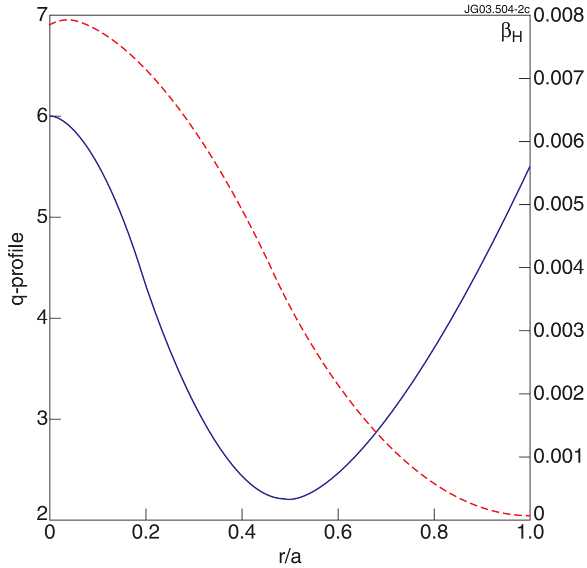

Figure 2: Radial profile for q (solid line) and β_H (broken line) for Pulse No: 49382 at 3.5<t(s)<4.0.

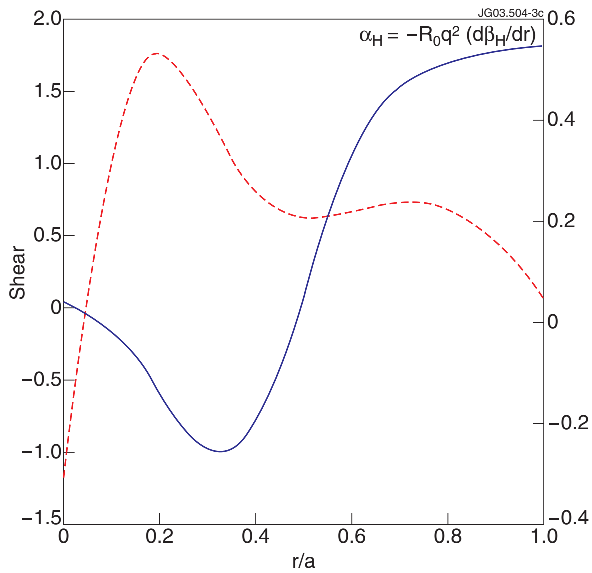

Figure 3: Radial profile for s=rq'/q (solid line) and αH (broken line) for Pulse No: 49382 at 3.5<t(s)<4.0.

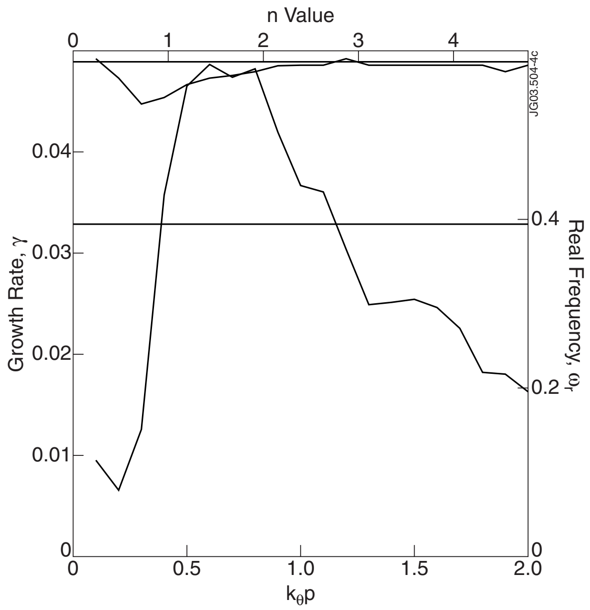

Figure 4: EPM growth rate γ (full line) and frequency ω_r (dotted line) at r/a=0.2. The TAE gap is also shown.

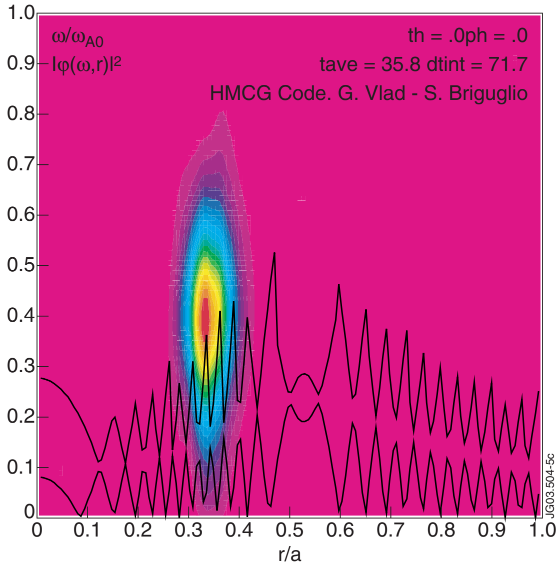

Figure 5: Contour plot for EPM amplitude in the (r/a,ω) plane in the linear destabilization phase at t=35.8τ_A.

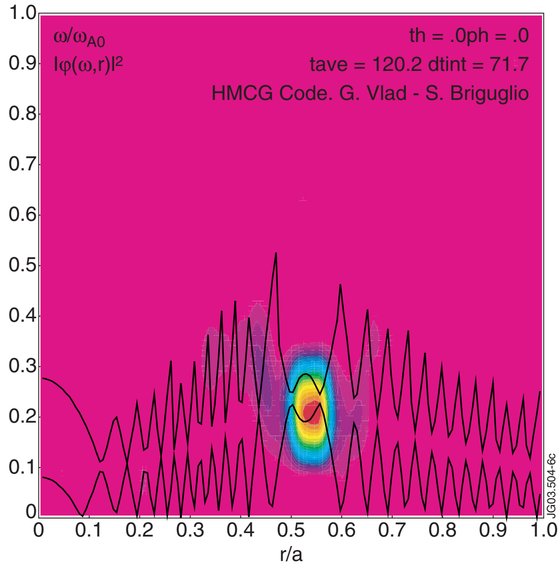

Figure 6: Same as Fig.5 but at t=120.2τ_A, in the nonlinearly saturated phase.